ELSEVIER

Journal of Chromatography A, 893 (2000) 359–366

JOURNAL OF CHROMATOGRAPHY A

www.elsevier.com/locate/chroma

Investigation of the nematic–isotropic transition of a liquid crystalline polymer and determination of molecular diffusion coefficients using gas chromatography

F. Gritti[a,b], G. Félix[a,*], M.-F. Achard[b], F. Hardouin[b]

[a]*E.N.S.C.P.B., Avenue Pey-Berland (BP 108), 33402 Talence, France*

[b]*C.R.P.P., Université Bordeaux I, Avenue A. Schweitzer, 33600 Pessac, France*

Received 27 April 2000; received in revised form 22 June 2000; accepted 7 July 2000

Abstract

Inverse gas chromatography has been used to study the nematic–isotropic transition of a side chain liquid crystalline polymer (LCP). The mesogenic side groups are laterally attached to a polysiloxane backbone through a flexible spacer. The nematic–isotropic transition of this LCP coated onto a glass capillary column is detected by considering the variation with temperature of the retention volume and of the theoretical plate number for the several probes. The molecular diffusion coefficients, *D*, of naphthalene, fluorene, pyrene and *o*-terphenyl have been determined at different temperatures in the nematic phase of the LCP as well as in the isotropic melt. The values ranged between 10^{-14} and 10^{-12} m^2 s^{-1} for the polynuclear aromatic hydrocarbon probes tested. © 2000 Elsevier Science B.V. All rights reserved.

Keywords: Inverse gas chromatography; Capillary columns; Liquid crystalline stationary phases; Retention volumes; Diffusion coefficients; Polynuclear aromatic hydrocarbons

1. Introduction

The use of low-molecular-mass (low-M_r) liquid crystals as an analytical tool was first reported in the 1960s by Kelker [1] and Dewar and Schröeder [2] in gas chromatography (GC). Since then, liquid crystalline polymers (LCPs) have substituted the low-M_r liquid crystals [3–9] because they offered both better thermal stability and column efficiencies.

GC has also been carried out to determine several properties of LCPs [10–16], including transition temperatures, degree of crystallinity and thermodynamic parameters such as activity coefficients, excess enthalpies, and enthalpies of solution at infinite dilution. This application of GC is called inverse gas chromatography (IGC).

Other information obtained by IGC concerns the solute diffusion coefficient at different temperatures in the liquid phase of a chromatographic column. Measurements of the diffusion coefficients in liquid crystals were usually achieved by direct methods like tracer techniques [17–19] or indirect methods like quasi-elastic neutron scattering (QENS) [20,21] as well as nuclear magnetic resonance (NMR) [22,23]. Seldom was their determination using IGC: for

*Corresponding author. Tel.: +33-5-5684-6561; fax: +33-5-5796-2239.

0021-9673/00/$ – see front matter © 2000 Elsevier Science B.V. All rights reserved.
PII: S0021-9673(00)00772-X

example, Grushka and Solsky [24,25] determined the molecular diffusion coefficient of *ortho*- and *para*-xylene in 4,4′-dimethoxyazoxybenzene (PAA) and *p*-(*p*-ethoxyphenylazo)phenyl-undecylenate (EPAP-U) low-M_r liquid crystals. In the same way Medina [26,27] measured diffusion coefficients of xylene isomers in the successive mesophases of 4,4′-bis(heptyloxy)azoxybenzene (BHOAB), and of picoline isomers in the smectic, cholesteric and isotropic phases of cholesteryl myristate low-M_r liquid crystals.

Thus, from our knowledge, no diffusion coefficient of probes in liquid crystalline polymers has been determined with IGC on a glass capillary solid support. Herein, we use a side-chain LCP, with the mesogenic side groups laterally attached to the polymer backbone through a flexible spacer. The polymer $P_{10.4.4}$ exhibits a nematic mesophase. Note that we have recently reported new stationary phases for high-performance liquid chromatography (HPLC) based on similar side-chain LCP with a lateral fixation. These phases showed excellent planarity and rod shape recognition capabilities and better performances than the corresponding LCP with a longitudinal fixation [28].

The first goal of this study was to investigate the influence of the phase nature of this LCP (nematic or isotropic liquid) on both the specific retention volume and theoretical plate number. Secondly, we used these results to determine the variation of the molecular diffusion coefficients of naphthalene, fluorene, pyrene and *o*-terphenyl with temperature in order to approach the specific interactions between liquid crystalline phases and molecular shape of the solutes.

2. Experimental

2.1. Chemicals

The polycyclic aromatic hydrocarbons (PAHs; naphthalene, fluorene, pyrene and *o*-terphenyl) used as solutes in this study were all of reagent grade and obtained from Aldrich–Sigma (L'Isle d'Abeau Chesnes, France). Polymethylhydrogenosiloxane (PHMS 67) was purchased from ABCR (Karlsruhe, Germany). All other compounds required for the synthesis of the liquid crystalline material were purchased from Aldrich–Sigma.

2.2. Liquid crystalline material

The LCP used in this work belongs to the family of the side-chain liquid crystalline polymer where the mesogenic rod-like units are laterally attached to a flexible polysiloxane backbone via a long spacer containing 10 methylene groups ($P_{10.4.4}$ for short):

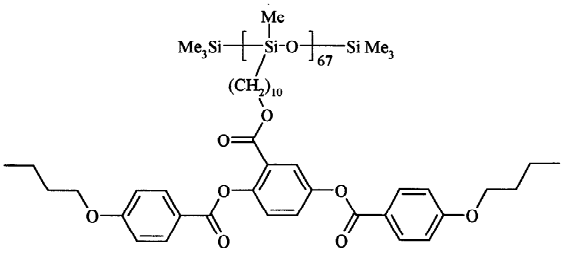

2.3. Mesogenic unit

The mesogenic group is of the three-phenyl ring benzoate type with terminal alkoxy chains. It is a vinyl derivative from the unsaturated termination of the spacer chain which is laterally fixed on the rod-like moiety. It is labeled $M_{n.m.m}$ where n and m are the number of carbons of the lateral alkyl ester spacer arm and of the alkoxy terminal chains, respectively. In our study, $n=10$ and $m=4$. The synthetic method of the mesogenic compounds $M_{n.m.m}$ has been previously described [29].

2.4. Liquid crystal homopolysiloxanes

The liquid crystal homopolysiloxane derived from the $M_{10.4.4}$ unit is named $P_{10.4.4}$. It is prepared through a classical hydrosilylation reaction [30,31] between the silane functions of the polymethylhydrogenosiloxane and the vinyl terminations of the spacer arm of the $M_{10.4.4}$ precursors. When all silane functions have reacted, the so-called homopolysiloxane is obtained.

Transition temperatures of the polymer were determined by differential scanning calorimetry (DSC) on a Perkin-Elmer DSC7 apparatus using heating rate of 10°C min^{-1}. The nematic–isotropic transition temperature corresponds to the maximum of the heat

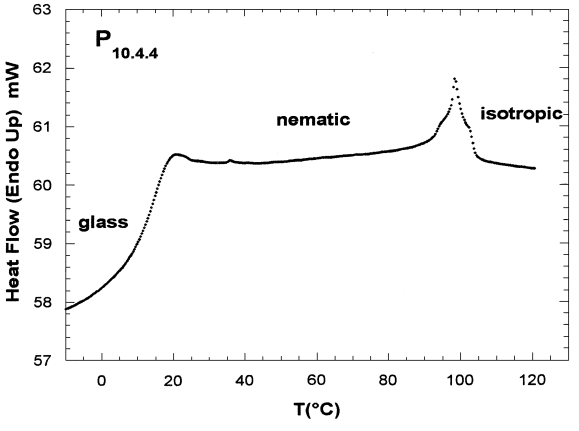

Fig. 1. DSC thermogram for $P_{10.4.4}$ liquid crystalline polymer. Heating rate 10°C min^{-1}.

peak on the thermogram (Fig. 1). Nevertheless, as expected for the polymolecularity of a polymer, the transition range (94–102°C) is larger than for a low-M_r compound. The enthalpy change associated with the nematic–isotropic transition is weak ($\Delta H \approx$ 1.5 J g^{-1}) and this low value traduces a weakly first-order transition:

$$\text{Glassy} \overset{17^{\circ}C}{\rightarrow} \text{Nematic} \overset{98^{\circ}C}{\rightarrow} \text{Isotropic}$$

2.5. Preparation of the capillary column

The preparation of the coated capillary column used the static method: the $P_{10.4.4}$ liquid crystalline polymer obtained was dissolved in dichloromethane previously dried over a 4-Å molecular sieve. The concentration was fixed at 2 mg ml^{-1} and the solution was degassed in an ultrasonic bath with the application of a slight vacuum. The capillary column (17 m×200 μm I.D. fused-silica) was purchased from Cluzeau Info Labo (Sainte-Foy-la-Grande, France). It was filled with the help of a slight vacuum applied at one end while the other end was plunged in the liquid crystal polymer solution. The filled capillary was then closed at one end with wood glue and plunged in a water bath thermostated at 22°C leaving the open end out of the bath. The solvent evaporation lasted 48 h. Finally, the capillary column was heated up to 130°C progressively under carrier gas flow in order to evacuate any traces of dichloromethane or volatile impurities.

2.6. Apparatus

An Intersmat Model 120 FB gas chromatograph equipped with flame ionization detection was used. The oven temperature was controlled to a precision of 0.3°C. The column was equilibrated for 15 min for each temperature increment. The inlet pressures of carrier gas, were measured with a mercury manometer. The flow-rate of nitrogen carrier gas was measured at room temperature and atmospheric pressure with a soap bubble flow meter. Sample injection volumes of 0.1 μl were added using a Hamiltonian syringe of 1 μl. The chromatograms were recorded on an Intersmat integrator–calculator–recorder, Model ICR-1B and the retention times were measured to a precision of 0.1 s. The mean of at least three consecutive readings agreeing to within 1% was taken. The half-height peak width was measured with a Peak Lupe (Scale 7X).

3. Results and discussion

3.1. Observation of the nematic–isotropic transition temperature of the LCP

As it has already been seen on a side-chain LCP with the mesogenic groups longitudinally attached [32,33], it appeared possible to determine the clarification temperature of the polymer by IGC. Nevertheless, considering the specific retention volume V_R, the authors observed a wider temperature range in V_R change at the transition than seen for the low-M_r liquid crystal, due to the polydispersity of a liquid crystalline polymer.

In the case of our laterally attached LCP, the investigation of the nematic–isotropic transition was only possible since the glassy–nematic phase change at 17°C was too low to allow the solutes to cross the 17 m length column.

The fundamental aspect of the IGC technique is the measurement, under accurately controlled conditions, of the chromatographic retention times for various solutes over the polymer coated onto the capillary column. In order to compare the retention times of each solute, the specific retention volume V_R [34] was calculated because the inlet pressure of the gas may be different from one solute to another. V_R

corresponds to the volume of the carrier gas at standard temperature and pressure per gram of polymer required to elute a component from the column:

$$V_R = F(t_R - t_0)/w$$

where t_R and t_0 are the retention times of the solutes and the hold-up time, respectively, w is the weight of polymer ($w = 1.07$ mg) and F is the flow-rate of the carrier gas corrected to 273.2 K and atmospheric pressure P_0. The latter is calculated as follows:

$$F = F'\left(\frac{273.2}{T_f}\right)\cdot\left(\frac{P_0}{760}\right)\cdot\left(\frac{P_0 - P_w}{P_0}\right)\cdot\left[\frac{3}{2}\cdot\left(\frac{(P_i/P_0)^2 - 1}{(P_i/P_0)^3 - 1}\right)\right]$$

where F' is the flow-rate of carrier gas measured at the outlet of the column at the temperature T_f and under atmospheric pressure P_0 (measured in Torr; 1 Torr = 133.322 Pa). P_w is the partial vapor pressure of water in the flow meter and P_i the carrier gas pressure at the column inlet. The last term takes into account the gas compressibility when it passes through the capillary column. As our nitrogen carrier gas was dried beforehand, $P_w = 0$.

The value of t_0 is calculated with respect to the Darcy law applied for capillary column:

$$\bar{u} = \frac{r^2}{8\eta}\cdot\frac{\Delta P}{L_c};\ t_0 = \frac{L_c}{\bar{u}}$$

where $\bar{u}$ is the carrier gas mean velocity, r the internal radius of the capillary column ($r = 0.1$ mm), η the carrier gas viscosity taken at 373 K (nitrogen, $\eta = 2.1\cdot10^{-5}$ kg m^{-1} s^{-1}), ΔP the differential pressure between the inlet and outlet pressures and L_c the capillary column length.

The retention diagrams presented in Fig. 2 are plotted as the variation of $\ln V_R$ with $1/T$, where T is the temperature (K). The slope of the linear portion of the experimental curve is given by:

$$\frac{d\ln V_R}{d1/T} = -\frac{\Delta H_s^\infty}{R}$$

where ΔH_s^∞ is the heat of solution of the probe at infinite dilution in the stationary phase and R the molar gas constant.

This linear evolution is observed when the coated

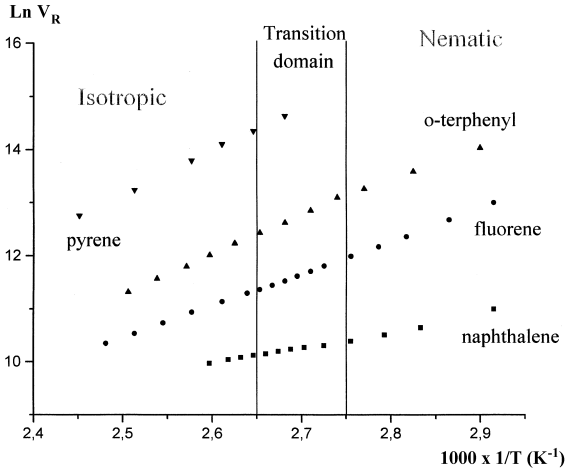

Fig. 2. Retention diagrams for $P_{10.4.4}$ LCP: (■) naphthalene, (●) fluorene, (▲) *o*-terphenyl, (▼) pyrene.

stationary phase remains in the same thermodynamic state. When a phase transition occurs (melting, glass transition or nematic–isotropic transition) generating a structure change for the stationary phase, a break in the linear variations appears. When the temperature increase, the stationary phase ordering decreases and retention volumes slightly change until all the more ordered phase is transformed into the less ordered one. Then a new linear evolution is again observed. Herein, the nematic–isotropic temperature of the $P_{10.4.4}$ polymer can be seen as change in the slope for all the probes. In addition, the determined transition temperature appears independent of the probe used. Furthermore, the gap at the transition temperature between the two Van 't Hoff linear domains is very small and never exceeds 0.2 logarithm units. As a comparison, Price and Shillcock obtained a similar value for the smectic–isotropic transition of their LC copolymer [32]. Of course, it is largely inferior to the gap measured at the melting transition of a low-M_r liquid crystal (which is a strongly first-order transition) where a change larger than one logarithm unit is detected. As observed by DSC, this IGC experiment confirms that the nematic–isotropic transition is slightly first order because the observed discontinuity is rather small. Through these retention diagrams, the nematic–isotropic transition appears quasi continuous and this behavior also traduces an enlarged

transition domain due to the polymolecularity of this high-molecular-mass material.

It is also interesting to note on Fig. 2 that for planar solutes, the Van 't Hoff linear domain corresponding to the isotropic phase is located above the extrapolation of the nematic linear domain. It would suggest that a planar probe presumably penetrate the nematic structure with slightly greater difficulty than the isotropic liquid. A reversed behavior is observed for the non-planar *o*-terphenyl probe: in this case, the flexibility of this molecule probably favors its penetration in the nematic structure.

Also important to note are the respective slopes of each linear portion (Fig. 2), which corresponds to ΔH_s^{∞} either in the nematic state or in the isotropic melt of the stationary phase (Table 1). This slope is slightly lower in the isotropic state than in the nematic and the inverse is observed for the *o*-terphenyl probe: from the Van 't Hoff equation, for planar solutes, the differential enthalpy of dissolution ΔH_s^{∞} between the LCP phase and the nitrogen gas phase is less negative with the isotropic melt than with the more ordered nematic phase and inversely for *o*-terphenyl. These experimental data agree with the fact that planar solutes better interact with more ordered phases, like liquid crystalline phases, than with a disordered liquid. A reversed tendency is observed for non-planar solutes. These observations illustrate the results obtained by Jinno et al. [35] in HPLC with 2,4,6-(triterbutylphenoxy)dimethyl (TBP) or benzyldimethyl (benzyl) bonded silica phases compared to a typical octadecylsilica (ODS) phase. The former two are not akin to an ordered liquid crystal phases and the latter is a more likely ordered phase. The authors observed that non-planar solutes were retained longer on TBP and benzyl phases than their homologous planar solutes, while the non-planar solutes are eluted before the planar ones on an ODS phase as well as on a LCP stationary phase [28].

The nematic–isotropic transition visible in the retention diagrams of Fig. 2, can be revealed with a better precision when considering the efficiency of the capillary column. The efficiency is quantified by the theoretical plate number *N*, experimentally measured for one solute as follows:

$$N = 5.54 \cdot \left(\frac{t_R}{\delta}\right)^2$$

where t_R is the probe retention time and δ the half-height peak width. In Figs. 3 and 4 the variations of *N* with the temperature of the column for each probe are presented. It is obvious that *N* is more sensitive to the phase transition of liquid crystalline polymer than the specific retention volume. For naphthalene, in the isotropic phase *N* is at least four-times this observed in the nematic one. For the planar probes, the lower the molecular mass of the probe, the higher the column efficiency and the more pronounced its variation occurring during phase change; thus, it becomes easier to localize the transition temperature by comparison with retention diagrams' method. For example, transition temperatures of 99°C, 101°C, 103°C (±2°C) are deduced from column efficiency data obtained with naphthalene, fluorene and *o*-terphenyl probes, respective-

Table 1
Heat of solution at infinite dilution and activation energies associated with the diffusion process in the nematic phase and in the isotropic melt of the $P_{10.4.4}$ LCP

Structure	Probes	Size V_m (Å^3)[a]	Shape L/B[b]	Heat of solution at infinite dilution (kJ mol^{-1})		Activation energy (kJ mol^{-1})	
				$\Delta H_s^{\infty\ \text{isotropic}}$	$\Delta H_s^{\infty\ \text{nematic}}$	$E_A^{\text{isotropic}}$	E_A^{nematic}
Planar	Naphthalene	126	1.24	−25	−32	32	40
	Fluorene	162	1.52	−51	−54	30	68
	Pyrene	185	1.26	−70	n.d.[c]	18	n.d.[c]
Non-planar	*o*-Terphenyl	225		−62	−40	24	17

[a] Static molecular volume (Van der Waals) calculated by molecular mechanic on a MacroModel program.
[b] Length-to-breath ratio given by Sander and Wise [39].
[c] Value non-detectable.

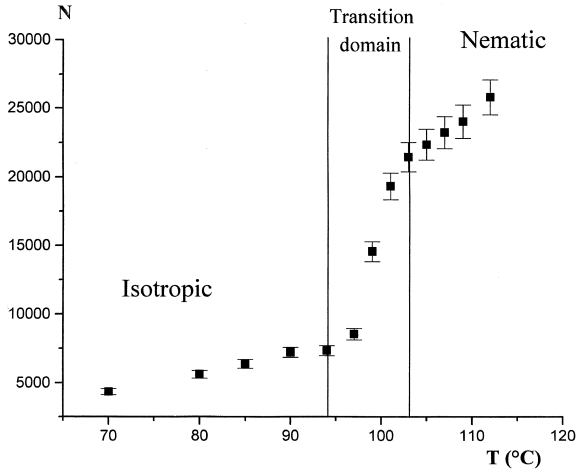

Fig. 3. Theoretical plate numbers N for $P_{10.4.4}$ LCP with naphthalene solute.

ly. Although retention times of pyrene were not available under 100°C (an excessively long time giving rise to no distinguishable peak) the column efficiency data also confirms the existence of the nematic–isotropic transition around 100°C.

The explanation of this large efficiency breaking at the transition temperature is contained in the Golay equation [36] (derived from the Van Deemter equation [37]) proposed to describe the influence of the carrier gas mean velocity on the equivalent height to a theoretical plate (H) for capillary columns:

$$H = \frac{B}{\bar{u}} + C_G\bar{u} + C_L\bar{u}$$

where $\bar{u}$ is the carrier gas mean velocity and B, C_G, C_L are given by the following equations:

$$B = 2D_G$$

$$C_G = \frac{r^2}{D_G} \cdot \frac{1 + 6k + 11k^2}{24(1+k)^2}$$

$$C_L = \frac{e_f^2}{D_L} \cdot \frac{2k}{3(1+k)^3}$$

$$k = \frac{t_R - t_0}{t_R}$$

where B is the longitudinal diffusion coefficient at unit pressure, C_G is the mass transfer resistance in the gas phase, and C_L the mass transfer resistance in the liquid phase and k the capacity factor. In these equations, r is the internal radius of the capillary column, D_G the molecular diffusion coefficient of the probe in the gas phase at unit pressure, D_L the molecular diffusion coefficient of the probe in the liquid phase and e_f the thickness of the polymer film.

In our experiments $\bar{u}$, r, e_f and D_G are supposed to be constant along the applied temperature range (343–413 K). D_G values have been obtained from those given in air [38] at 298 K after correction at 100°C. Using a hard sphere model, the molecular diffusion coefficient of a solute in gas varies as $T^{3/2}$ giving rise to corrected factor of 1.32 to obtain the value at 413 K from that at 343 K. Variation of the density of the LCP is neglected so the film thickness remains the same over the whole temperature range. Consequently, the only terms susceptible to important variation with temperature are the capacity factor k and the molecular diffusion coefficient D_L that may change when the LCP structure change occurs. The accelerated increase of N when the polymer passes from the nematic to the isotropic state would therefore be explained by the higher probe diffusivity in the isotropic state, decreasing the mass transfer resistance C_L in the liquid phase and also increasing the capillary column efficiency N.

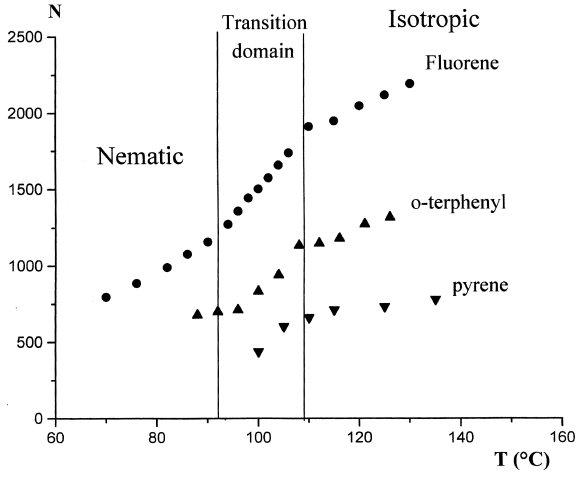

Fig. 4. Theoretical plate numbers N for $P_{10.4.4}$ LCP: (●) fluorene, (▲) *o*-terphenyl, (▼) pyrene.

3.2. Determination of the molecular diffusion coefficient D_L of PAH solutes in LCP phases

It is possible to calculate D_L as a function of the temperature from the Golay equation:

$$D_L(T) = \frac{\frac{2}{3}\cdot e_f^2\bar{u}\cdot\frac{k(T)}{[1+k(T)]^2}}{H(T) - \frac{2D_G}{\bar{u}} - \frac{r^2\bar{u}}{D_G}\cdot\frac{1+6k(T)+11k(T)^2}{24[1+k(T)]^2}}$$

The variations of the molecular diffusion coefficient of naphthalene, fluorene, pyrene and *o*-terphenyl, as a function of the reciprocal temperature are given in Fig. 5. The diffusion coefficients sharply change as the liquid crystalline polymer becomes isotropic. For all solutes, D_L are lower in the nematic phase than in the isotropic state (nevertheless, note that near the transition temperature the values determined in the isotropic phase never exceed five-times those obtained in the nematic phase). At a phase transition, smaller D_L values are generally observed in the low-temperature phase but the opposite jump has also been seen [27].

In each phase of the LCP, isotropic or nematic, the relation between the diffusion coefficient and temperature is given by a simple Arhenius behavior:

$$D_L = D_L^* \exp(-E_A/RT)$$

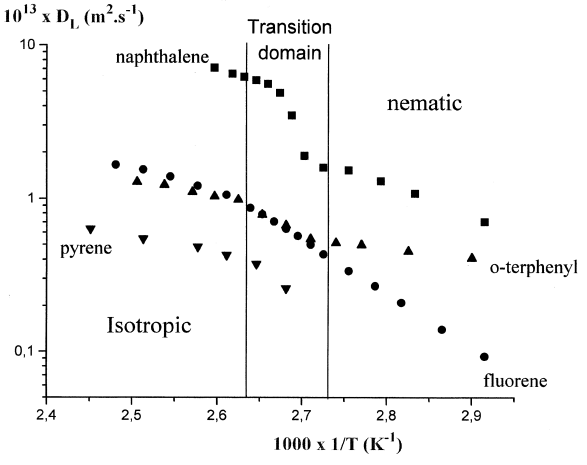

Fig. 5. Molecular diffusion coefficient D_L of solutes in $P_{10.4.4}$ LCP: (■) naphthalene, (●) fluorene, (▲) *o*-terphenyl, (▼) pyrene.

where D_L^* denotes a fitting parameter and E_A is the activation energy per mole of solute necessary to jump from one diffusion site to another.

The calculated molecular diffusion coefficients are ranged between 10^{-14} and 10^{-12} m^2 s^{-1} for pyrene, *o*-terphenyl, fluorene and naphthalene molecules on our liquid crystalline polymer. These values are clearly lower than those determined by the same technique on low-M_r liquid crystals for small aromatic compounds [24–27]. For example, Medina [27] found for xylene and picoline isomers diffusion coefficients comprised between 10^{-10} and 10^{-9} m^2 s^{-1} on the cholesteryl myristate liquid crystal. It is interesting to compare the values obtained for the same probe (*o*-xylene) on two different low-M_r liquid crystals on the cholesteryl myristate, which is on a non-aromatic low-M_r compound, $D_L \approx 2\cdot10^{-10}$, $3\cdot10^{-10}$ and $1\cdot10^{-10}$ m^2 s^{-1} in the isotropic, cholesteric and smectic phases, respectively while on a two phenyl ring low-M_r liquid crystal (PAA), lower values are obtained ($4\cdot10^{-11}$ m^2 s^{-1} in the nematic phase and $7\cdot10^{-11}$ m^2 s^{-1} in the isotropic melt [24]) traducing better interactions of *o*-xylene with an ''aromatic'' stationary phase.

In our case, stronger $\pi-\pi$ interactions between the three phenyl rings of the LCP stationary phase and polyaromatic probes, larger hydrophobic interactions as well as the higher viscosity of LCP over low-M_r liquid crystals might explain the low D_L values obtained.

Diffusion coefficients depend on numerous factors: the viscosity and density of the solvent, the diffusion path of the probe taken in the liquid phase during the diffusion process, the size and shape of the probe and the interactions between solvent and probe. With liquid crystalline stationary phase, Medina [27] showed that, the diffusivity of isomers in a smectic structure also depends on the molecular shape (in terms of length-to-breath ratio). In our case, the PAH probes used are not isomers, and thus the specific influence of the molecular shape cannot be quantitatively evaluated. Nevertheless several comments can be made:

(1) As expected, for the set of planar solutes, the lower the probe molecular volume, the higher the D_L and this order is maintained in the nematic phase:

$$D^{\text{isotropic}}_{\text{naphthalene}} > D^{\text{isotropic}}_{\text{fluorene}} > D^{\text{isotropic}}_{\text{pyrene}}.$$

Nevertheless, for non-planar *o*-terphenyl solute, although it is heavier than pyrene, its molecular diffusion coefficient is superior to pyrene.

(2) The activation energies associated with the diffusion path taken by the probes in the nematic phase are largely increased when comparing naphthalene ($L/B=1.20$, $E_A=40$ kJ mol^{-1}) with fluorene ($L/B=1.50$, $E_A=68$ kJ mol^{-1}). Although they were quite identical in the isotropic phase (32 and 30 kJ mol^{-1}). A discrimination thus appears in the nematic phase with regard to the solutes' elongated shape features.

(3) The probe planarity is also important. Despite the fact that *o*-terphenyl and fluorene have comparable D_L in the isotropic state, the diffusivity of *o*-terphenyl becomes clearly higher than for fluorene in the nematic state:

$$D^{\text{isotropic}}_{o\text{-terphenyl}} \cong D^{\text{isotropic}}_{\text{fluorene}}; D^{\text{nematic}}_{o\text{-terphenyl}} > D^{\text{nematic}}_{\text{fluorene}}.$$

This confirms that non-planar solutes interact less with ordered phases than the planar solutes do. The activation energy decreases for *o*-terphenyl but strongly increases for fluorene when the LCP passes from the isotropic to the nematic state. In the nematic state, activation energies' range is largely widen and they vary from 16 kJ mol^{-1} for *o*-terphenyl up to 68 kJ mol^{-1} for the more elongated probe (fluorene), marking the higher sensitivity of the ordered nematic phase over the disordered isotropic with respect to the solutes' shape.

References

[1] H. Kelker, Z. Anal. Chem. 198 (1963) 254.
[2] M.J.S. Dewar, J.P. Schröeder, J. Am. Chem. Soc. 86 (1964) 5235.
[3] H. Finkelmann, R.J. Laub, W.L. Roberts, C.A. Smith, in: M. Cooke, A.J. Dennis, G.L. Fisher (Eds.), Polynuclear Aromatic Hydrocarbons – Physical and Biological Chemistry, Battele Press, Columbus, OH, 1982, p. 275.
[4] G.M. Janini, R.J. Laub, J.H. Purnell, in: C.B. McArdle (Ed.), Side-Chain Liquid Crystal Polymers, Blackie Press, Glasgow, London, 1989, p. 395.
[5] Z. Witkiewicz, J. Chromatogr. 466 (1989) 37.
[6] Z. Witkiewicz, J. Mazur, LC·GC 8 (1990) 224.
[7] K.P. Naikwadi, A.L. Jadhav, S. Rokushika, H. Hatano, M. Ohshima, J. Makromol. Chem. 187 (1986) 1407.
[8] A.L. Jadhav, K.P. Naikwadi, S. Rokushika, H. Hatano, M. Ohshima, J. High Resolut. Chromatogr. Chromatogr. Commun. 10 (1987) 77.
[9] S. Rokushika, K.P. Naikwadi, A.L. Jadhav, H. Hatano, J. High Resolut. Chromatogr. Chromatogr. Commun. 8 (1985) 480.
[10] S. Ghodbane, G.A. Oweimreen, D.E. Martire, J. Chromatogr. 556 (1991) 317.
[11] D.E. Martire, P.A. Blasco, P.F. Carone, L.C. Chow, H. Vincini, J. Phys. Chem 72 (1968) 3489.
[12] H.-J. Moegel, G. Kraus, M. Novak, J. Chromatogr. 324 (1985) 29.
[13] J. Coca, I. Medina, S.H. Langer, Chromatographia 25 (1988) 825.
[14] G.A. Oweimreen, Mol. Cryst. Liq. Cryst. 68 (1980) 257.
[15] G.A. Oweimreen, A.-K.I. Shihab, J. Chem. Eng. Data 266 (1994) 39.
[16] G.J. Price, I.M. Shillcock, Can. J. Chem. 73 (1995) 1883.
[17] T. Svedberg, Kolloidzeitschrift 82 (1918) 68.
[18] C.K. Yun, A.G. Fredrickson, Mol. Cryst. Liq. Cryst. 12 (1970) 73.
[19] A.V. Chadwick, M. Paykary, Mol. Phys. 39 (1980) 637.
[20] J. Töpler, B. Alefeld, T. Springer, Mol. Cryst. Liq. Cryst. 26 (1973) 297.
[21] M. Bée, A.J. Dianoux, J.A. Dianik, J.M. Janik, R. Podsiadly, Liq. Cryst. 10 (1991) 199.
[22] G.J. Krüger, Phys. Rep. 82 (1982) 229.
[23] F. Noack, Mol. Cryst. Liq. Cryst. 113 (1974) 247.
[24] E. Grushka, J.F. Solsky, Anal. Chem. 45 (1973) 1836.
[25] E. Grushka, J.F. Solsky, J. Chromatogr. 112 (1975) 145.
[26] I. Medina, Chromatographia 35 (1993) 539.
[27] I. Medina, Liq. Crystals 12 (1992) 989.
[28] I. Terrien, M.-F. Achard, G. Félix, F. Hardouin, J. Chromatogr. A 810 (1998) 19.
[29] P. Keller, F. Hardouin, M. Mauzac, M.-F. Achard, Mol. Cryst. Liq. Cryst. 155 (1988) 171.
[30] M. Mauzac, F. Hardouin, H. Richard, M.-F. Achard, G. Sigaud, H. Gasparoux, Eur. Polym. J. 22 (1986) 137.
[31] G. Gray, J.S. Hill, D. Lacey, Angew. Chem. Int., Educ. Engl. Adv. Mater. 28 (1989) 1120.
[32] G.J. Price, I.M. Shillcock, Polymer 34 (1993) 85.
[33] G.J. Price, I.M. Shillcock, Polym. Mater. Sci. Eng. Washington 70 (1994) 419.
[34] J.R. Conder, C.L. Young, Physicochemical Measurement By Gas Chromatography, Wiley, Chichester, 1978.
[35] K. Jinno, C. Okumura, M. Harada, Y. Saito, J. Liq. Chromatogr. Rel. Technol. 19 (1996) 2883.
[36] M.J.E. Golay, in: D.H. Desty (Ed.), Gas Chromatography 1958, Butterworth, London, 1958, p. 36.
[37] J.J. Van Deemter, F.J. Zuyderweg, A. Klinkenberg, Chem. Eng. Sci. 5 (1956) 271.
[38] J. Perry, Chemical Engineer's Handbook, McGraw Hill (Eds.) (1950) 538.
[39] L.C. Sander, S.A. Wise, Polycyclic Aromatic Hydrocarbon Structure Index, NIST Special Publication, No. 922, 1997.